

Reaction Behavior of Biodegradable, Photo-Cross-Linkable Polyanhydrides

Dina Svaldi Muggli,[†] Amy K. Burkoth, Sarah A. Keyser, Hyun R. Lee, and Kristi S. Anseth*

Department of Chemical Engineering, University of Colorado, Boulder, Colorado 80309-0424

Received January 27, 1998; Revised Manuscript Received April 13, 1998

ABSTRACT: The polymerization behavior of a new class of dimethacrylated anhydride monomers that react to form highly cross-linked degradable networks was investigated using various photoinitiation schemes. Polymerizations occurred in seconds to minutes depending on the initiating conditions, and conversions in excess of 0.95 were achievable. A photobleaching visible light initiating system was used to improve the depth of cure for the production of polymers with appreciable dimensions. One potential application for the proposed multifunctional monomers is in vivo curing of high-strength, degradable polymers for fracture fixation or filling of trabecular bone defects.

Introduction

Numerous musculoskeletal applications would benefit from recent advances in the development of safe, strong, easily fashioned, and degradable polymers. For example, bone fractures are a major health concern, and in a study of musculoskeletal conditions in the United States, an estimated 6.3 million fractures occurred during a typical 3 year period.¹ The established standard for treatment for many of these fractures, especially those involving weight-bearing bones, is the use of metal plates for fixation.² Current limitations to metallic implants for fracture fixation include the following: stress-shielding during healing, which can lead to excessive bone resorption and osteoporosis; corrosion by a fairly aggressive electrolyte (0.9% NaCl), which can lead to chronic inflammation and is a problem to patients with metal sensitivity; and fatigue and loosening of the implant.³ Many of these issues, as well as others, necessitate a second surgery to remove the implant after healing, and the risk and expense to the patient is nontrivial. Hence, degradable polymeric materials provide an important alternative to metallic implants.

Degradable polymers eliminate the need for a second surgery and, if carefully designed, can prevent some of the problems associated with stress-shielding during healing. Additionally, degradable polymer implants can be used simultaneously to deliver therapeutic drugs to prevent or treat infections or growth factors to aid or accelerate in new bone growth. Furthermore, a recent workshop sponsored by the American Academy of Orthopaedic Surgeons and the National Institute of Arthritis and Musculoskeletal and Skin Diseases recommended that the development of new degradable polymer systems should be a major research priority.⁴

To this extent, we recently developed and investigated a class of photopolymerizable, methacrylate anhydride monomers, which react to form highly cross-linked polyanhydride networks for orthopedic applications.⁵ The rationale for the proposed polymer design was driven by several, critical factors. First, the number of

synthetic polymers approved by the FDA for human clinical studies is rather small, and of these, only three (poly(lactic acid), poly(glycolic acid), and poly(*p*-dioxanone)) are routinely applied in human medicine. The limitation to broader application of these polymers is linked to their bulk degradation. More recently, degradable linear polyanhydrides have been synthesized and gained FDA approval for the treatment of brain cancer.⁶ The combined hydrophobicity and the hydrolytic instability of the anhydride linkage lead to surface degradation in these polymers, which is advantageous for drug delivery (prevent dose dumping) and load-bearing applications (maintain polymer structural integrity).⁷

Second, we modified these anhydrides with photopolymerizable, methacrylate functionalities. Traditionally, methacrylate and acrylate based monomers have been widely used in the photopolymerization industry. Multifunctional methacrylate monomers form strong, hard polymers with excellent dimensional stability (i.e., minimal swelling). In addition, these functionalities have a long history in biomedical applications such as dental restorative materials and bone cements.⁸ Finally, the presence of a high degree of cross-linking in these networks facilitates improved mechanical properties and surface-controlled degradation. Because the cross-links themselves are anhydride linkages, the material remains biodegradable, and the rate of degradation is controlled by changing the composition of the polymer (to control hydrophobicity) and/or the molecular weight between photoreactive functionalities.

While the benefits of high-strength, biocompatible, and surface eroding materials are evident, development of a photopolymerizable system provides many additional advantages, including fast curing rates at room temperature, spatial control of the polymerization, and complete ease of fashioning and flexibility during implantation. Relatively few systems have been developed that can be reacted in vivo; they include redox-cured methyl methacrylate bone cements,⁸ injectable bioactive ceramic cements,⁹ photocured endocapsular lens replacements for cataract treatment,¹⁰ visible light-cured dental restorative materials,¹¹ and photocured hydrogels for uses in angioplasty to promote better healing.¹² In addition, many injectable gels are commercially avail-

* To whom correspondence should be addressed.

[†] Present address: RxKinetix, Inc., Louisville, CO 80027.

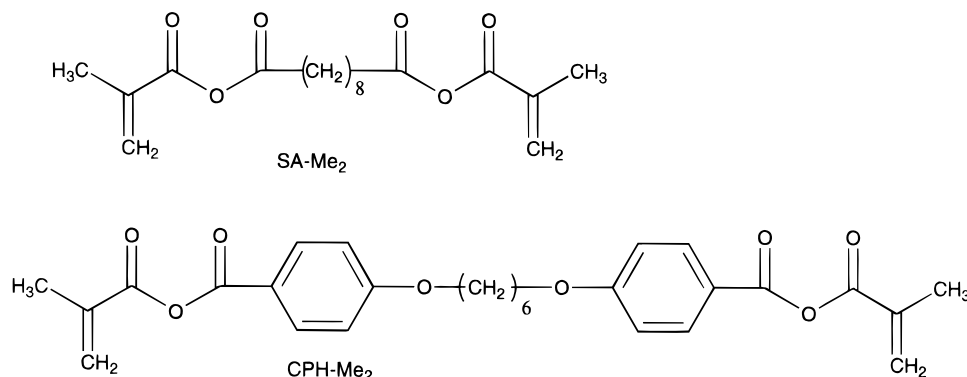


Figure 1. Chemical structures of methacrylated sebacic acid (SA-Me₂) and methacrylated 1,6-bis(carboxyphenoxy)hexane (CPH-Me₂).

able that undergo a physical gelation process (e.g., Pluronic) or ionic cross-linking (e.g., gelatin).¹³ One of the principal limitations to more extensive use of photopolymerizations in medicine is the lack of biocompatible monomers and/or oligomers that photopolymerize to form *degradable* polymer networks. Furthermore, outside of the newly developed photo-cross-linkable polyanhydrides, few systems are available that are photopolymerizable, are degradable, and achieve high-strengths. Each of these features is important in various orthopedics applications.

Polymerization conditions for *in vivo* applications are quite adverse, including a narrow range of physiologically acceptable temperatures, requirement for nontoxic monomers and/or solvents, moist and oxygen-rich environments, and clinically suitable rates of polymerization.¹⁴ Photoinitiations overcome many of these limitations, since the polymerization process is typically rapid (and can be controlled to occur over a time period of a few seconds to a couple of minutes), the fast polymerization rate can overcome oxygen inhibition and moisture effects, and polymerization does not require elevated temperatures. Thus, by selection or development of nontoxic monomers and/or solvents for orthopedic applications, these polymerization criteria may be met for *in vivo* curing.

Hence, the objective of this work was to examine the polymerization behavior of this newly developed class of dimethacrylated anhydrides under a variety of photoinitiation conditions to assess the feasibility of curing these monomers under simulated *in vivo* conditions. In particular, the rate of polymerization, the maximum functional group conversion, and the depth of cure were examined as a function of initiation type and conditions.

Experimental Section

Materials. Methacrylated sebacic anhydride (SA-Me₂) monomer (Figure 1) was synthesized from sebacic acid (Aldrich) and methacrylic anhydride (Aldrich). The SA-Me₂ was prepared by converting the dicarboxylic acid to an anhydride by refluxing in methacrylic anhydride for approximately 1 h. The dimethacrylated anhydride monomer was subsequently isolated and purified by dissolving in methylene chloride and precipitating in petroleum ether.

Dicarboxylic acid 1,6-bis(carboxyphenoxy) hexane (CPH) was synthesized as described elsewhere.¹⁵ To facilitate methacrylation of the less soluble CPH, the acid groups were first acetylated by refluxing in an excess of acetic anhydride (Aldrich) for several hours. The diacetylated CPH product was isolated and purified by washing in diethyl ether and vacuum filtering. The acetylated CPH was end-capped with methacrylate functionalities by refluxing in methacrylic anhydride

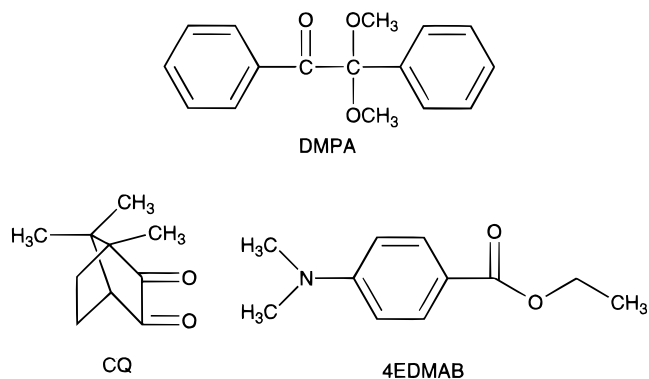


Figure 2. Chemical structure of various photoinitiators: 2,2-dimethoxy-2-phenyl acetophenone (DMPA), camphorquinone (CQ), and ethyl 4-*N,N*-dimethylaminobenzoate (4EDMAB).

for approximately 1 h. The dimethacrylated CPH monomer (CPH-Me₂, Figure 1) was subsequently isolated and purified by dissolving in methylene chloride and precipitating in petroleum ether. The methacrylated monomers were characterized with ¹H NMR and FTIR to examine the extent of methacrylation; The presence of =CH₂ protons in the methacrylate end-group was clearly evident as seen with ¹H NMR at approximately δ = 6.0 and δ = 6.5 ppm and with FTIR at approximately 1637 cm⁻¹.

Photopolymerizations were initiated with either ultraviolet (λ = 365 nm) or visible (λ = 470–490 nm) light. The ultraviolet initiator examined was 2,2-dimethoxy-2-phenylacetophenone (DMPA, Ciba Geigy), which is a standard photoinitiator used in many photopolymerization applications.¹⁶ UV-curable formulations were prepared by dissolving between 0.1 and 1.0 wt % of DMPA in the monomer being investigated. The visible light initiating system consisted of camphorquinone (CQ, Aldrich) and ethyl 4-*N,N*-dimethylaminobenzoate (4EDMAB, Aldrich). This visible light initiating system is typical in many current dental applications and provides an alternative to utilizing ultraviolet radiation to initiate polymerization.¹⁷ Samples of monomer with concentrations of CQ/4EDMAB varying between 0.2 wt %/0.8 wt %, and 1.0 wt %/1.0 wt % were investigated. All initiators were used as received, and initiator structures are shown in Figure 2.

Methods. All samples were polymerized with either full beam ultraviolet light (EFOS, Ultracure 100SS), longwave ultraviolet light (Black-Ray, Model B100AP, 115V, 2.5A), or a blue light (DenMat Marathon Two, Model 3940) curing system at various light intensities. Ultraviolet polymerizations were conducted with light intensities ranging from 1 to 150 mW/cm². Visible light polymerizations were performed at light intensities ranging from 30 to 150 mW/cm².

Polymerization rate profiles were monitored as a function of time using a differential scanning calorimeter equipped with a photocalorimetric accessory (DPC, Perkin-Elmer DSC7).

Neutral density filters (Melles Griot) were used to control the incident light intensity, and a monochromator was used to select the wavelength of the initiating light. Isothermal reaction conditions were maintained by an external recirculating chiller attached to the DSC cell. Generally, 8–12 mg of the monomer–initiator solution were placed in an aluminum DSC pan, and the polymerization rate was monitored at 37 °C in the presence of oxygen to simulate approximate *in vivo* conditions. The heat flux measured is directly proportional to the rate of polymerization, and the extent of double bond conversion can be calculated from the integrated peak area when the theoretical heat evolved per double bond is known.

Infrared spectroscopy (Nicolet Magna-IR 750 Series II) was used to monitor the polymerization behavior and final double bond conversion of the dimethacrylated anhydride monomers. Each monomer–initiator mixture was pressed into a thin film between polypropylene sheets and mounted on a holder. The thin films were photopolymerized, by exposure to light (UV or blue) of a measured intensity for a specified time period. The final double bond conversion in these samples was calculated based on the decrease in absorbance near 1637 cm^{-1} , a characteristic absorbance of the methacrylate double bond.¹⁸

Three-dimensional polymerization profiles were studied using attenuated total reflectance infrared spectroscopy (ATR-FTIR) to ascertain conversion as a function of depth for both UV (DMPA) and blue light (CQ/4EDMAB) initiator systems. Monomer samples of varying thickness were polymerized directly on a ZnSe crystal (45° incidence angle) by exposing the sample to a visible or UV light source for specified time periods. An ATR spectra of the sample was obtained following each irradiation period. For the polymer systems studied, the penetration depth was calculated to be approximately 700 nm at the surface in contact with the crystal. For both IR techniques, samples were polymerized under ambient conditions with oxygen present.

Results and Discussion

Both differential scanning photocalorimetry (DPC) and Fourier transform infrared spectroscopy (FTIR) were used to characterize the polymerization behavior, curing time, and maximum double bond conversion of the dimethacrylated anhydride monomers (SA-Me₂ and CPH-Me₂) under simulated *in vivo* conditions (i.e., in air and at ~37 °C). The purpose of these studies was to establish clinical curing times and to illustrate how initiating wavelength (UV or visible), initiator concentration, and incident light intensity can be used to control the conversion, polymerization rate, and curing time.

The effects of light intensity and initiator concentration on the UV-initiated polymerization of SA-Me₂ at 37 °C are shown in Figure 3. In general, the rate curves exhibited characteristics typical of multifunctional monomer polymerizations, showing an early onset of autoacceleration, which leads to a dramatic increase in the initial polymerization rate, followed by autodeceleration. The majority of double bonds were consumed within the first minute or two (depending on the initiating conditions), after which the polymerization rate became vanishingly small. The autoacceleration peak became more pronounced as higher initiator concentrations and higher light intensities were used. While the effects of initiator concentration and light intensity on the polymerization rate followed expected general trends, the results were complicated by the influence of volume relaxation (as will be discussed more thoroughly in Figure 4).

The significance of these results is 2-fold. First, the observed photopolymerization times are reasonable for a clinical setting, and second, the rate and time of

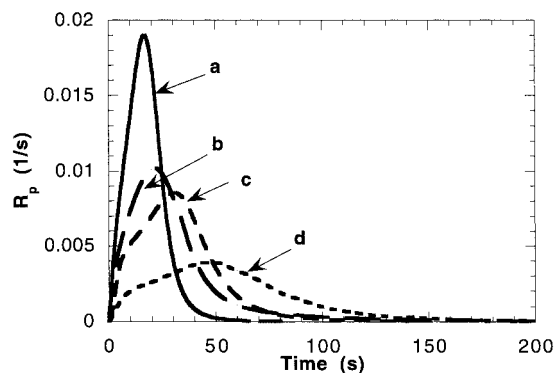


Figure 3. Effect of light intensity and initiator concentration on the rate of polymerization (R_p) vs time for the UV polymerization of SA-Me₂ at 37 °C: (a) 1.0 wt % DMPA, 150 mW/cm^2 ; (b) 0.1 wt % DMPA, 150 mW/cm^2 ; (c) 1.0 wt % DMPA, 7 mW/cm^2 ; (d) 0.1 wt % DMPA, 7 mW/cm^2 .

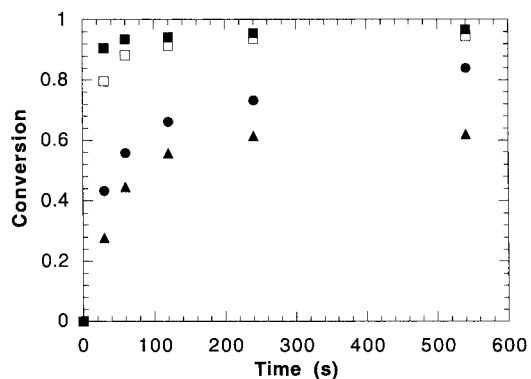


Figure 4. Effect of light intensity and initiator concentration on the UV polymerization of SA-Me₂: (■) 1.0 wt % DMPA, 150 mW/cm^2 ; (□) 1.0 wt % DMPA, 5 mW/cm^2 ; (●) 0.1 wt % DMPA, 150 mW/cm^2 ; (▲) 0.1 wt % DMPA, 5 mW/cm^2 .

polymerization can be controlled by adjusting the initiator concentration and/or light intensity. Of further interest is the double bond conversion reached in these systems, which was ambiguous to obtain from DPC results. First, the theoretical heat evolved per double bond for these dimethacrylated anhydrides has not been well-characterized. In addition, accurate determination of the concentration of double bonds in the monomer is difficult since oligomeric species are difficult to separate from the monomer.

Thus, FTIR studies were conducted to determine the maximum attainable double bond conversion and to elucidate further the clinical time necessary to cure the polymer. The effects of initiation rate and wavelength of the initiating light (i.e., 470–490 nm blue light or 365 nm UV light) on curing time and double bond conversion were investigated. These results are presented in Figures 4 and 5.

In Figure 4, the conversion profiles and final double bond conversions were determined under initiation conditions similar to those in the DPC studies. These results further illustrate the ability to control the curing time through changes in the initiation rate. For example, after 60 s of exposure to 150 mW/cm^2 of UV light, polymerization was complete in a system with 1.0 wt % initiator, whereas the system with 0.1 wt % initiator required over 200 s.

Additionally, the maximum functional group conversion attained in each system was 97% (1 wt % DMPA, $I_0 = 150 \text{ mW}/\text{cm}^2$), 96% (1.0 wt % DMPA, $I_0 = 5 \text{ mW}/\text{cm}^2$), 84% (0.1 wt % DMPA, $I_0 = 150 \text{ mW}/\text{cm}^2$), and 63%

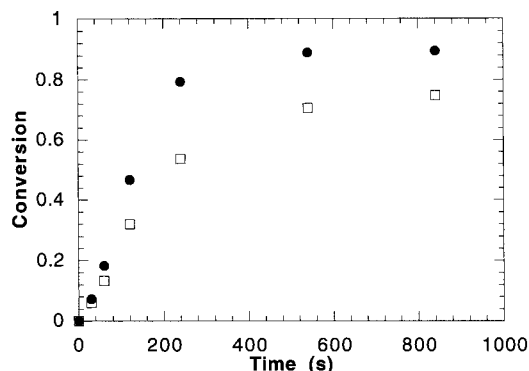


Figure 5. Effect of initiator concentration on visible light polymerization of SA-Me₂ at 150 mW/cm²: (●) 1.0 wt % CQ/1.0 wt % 4EDMAB; (□) 0.2 wt % CQ/0.8 wt % 4EDMAB.

(0.1 wt % DMPA, $I_0 = 5$ mW/cm²). Attainment of a maximum double bond conversion is typical in multifunctional monomer polymerizations and results from the severe restriction on bulk mobility of reacting species in highly cross-linked networks.¹⁶ In particular, radicals become trapped or shielded within densely cross-linked microgel regions, and the rate of polymerization becomes diffusion limited. Further double bond conversion is almost impossible at this point, and the polymerization stops prior to 100% functional group conversion. In polymeric dental composites, which use multifunctional methacrylate monomers, final double bond conversions have been reported ranging anywhere from 55 to 75%.¹⁹

If equal reactivity of the double bonds is assumed, only 0.09–13.7% of unreacted monomer (i.e., monomer with neither double bonds reacted) will be present at the highest and lowest final double bond conversions, respectively. Unreacted monomer can plasticize the polymer network, rendering it more pliable and decreasing its mechanical properties, and may also compromise the biocompatible nature of the system if the monomer leaches to a toxic level. Therefore, it is desirable to identify polymerization conditions that maximize the conversion of monomer.

In addition to attainment of a maximum double bond conversion, Figure 4 also shows the dependence of the final conversion on the initiation rate. Specifically, faster rates of initiation and polymerization lead to higher maximum double bond conversions (e.g., from 63% to 97%). This increase in conversion results from the effects of volume relaxation on the system mobility. In essence, polymerization occurs at a rate that surpasses the rate of volume shrinkage, creating excess free volume. This excess free volume leads to higher mobility of reacting species and, thus, higher conversions. Compared to linear polymer systems, volume shrinkage plays an increasingly important role in the kinetics of multifunctional monomer polymerizations, particularly since these systems tend to gel at very low double bond conversions, and form highly cross-linked networks that relax very slowly to equilibrium.²⁰

While the broad range of efficient initiators and availability of inexpensive UV lights have led to the wide use of UV-initiated polymerizations, many biomedical applications require or prefer the use of visible light. For example, dentistry uses blue light-initiated photopolymerizations to place polymeric composites in caries. The typical initiating system uses camphorquinone (CQ), ethyl-4-*N,N*-dimethylaminobenzoate (4EDMAB),

and 470–490 nm blue light. Considering its long-standing history in the dental community, this visible light-initiating system was chosen for these potential orthopedic polymers. Figure 5 contains FTIR results for the visible light polymerization of SA-Me₂ at two concentrations of CQ/4EDMAB initiated with 150 mW/cm² of blue light (i.e., a typical intensity from a standard dental curing unit).

The visible light polymerizations exhibited the same general dependence of the polymerization rate and final double bond conversion on the initiation rate as observed for the UV polymerizations. Specifically, increasing the initiator concentration led to higher polymerization rates and greater maximum conversions; however, the lower efficiency of this initiating system resulted in longer curing times and lower double conversions compared to the UV-initiated system. The efficiency is defined as the fraction of radicals formed in the primary step of initiator decomposition that are successful in initiating polymerization.²¹ The CQ/4EDMAB system generates radicals by hydrogen abstraction, which is generally less efficient than photocleavage, the mechanism by which DMPA generates radicals.²² However, the advantages of visible light over UV light include both safety and public perception. For example in a clinical setting, 5 mW/cm² represents a reasonable intensity for UV photopolymerizations (considering the average UVF of FDA approved tanning beds is 20 mW/cm²²³), while visible light intensities of 150 mW/cm² and greater are acceptable. Thus, visible light-initiated polymerizations offer a greater capability in controlling the polymerization time without increasing the initiator concentration.

All of the above studies pertained to a particular monomer system, specifically SA-Me₂. This material reacts to form a highly cross-linked network that surface erodes at a relatively rapid rate (e.g., disks 1 mm in thickness degrade in 48 h).²³ From a practical standpoint, it is desirable to develop networks where the degradation rate can be independently controlled. To achieve this control, a more hydrophobic monomer, CPH-Me₂, was synthesized that degrades much more slowly (e.g., disks 1 mm in thickness degrade in ~10 months).²³ Ideally, the network composition can be varied using these two monomers to produce polymers with degradation times ranging from a few days to nearly 1 year.

To produce such networks, an additional factor, which is the competitive absorption of the initiating light between the monomer and initiator, must be considered when selecting the initiator system and initiating wavelength. The issue of depth of cure also becomes increasingly relevant in applications requiring thick, 3D polymers (e.g., filling trabecular bone defects). While photopolymerizations are widely used in the fabrication of thin films, the production of thick 3D objects is more challenging because of absorption and scattering of the polymerizing light through the sample. Thus, ATR-FTIR was used to examine these issues, and the 3D cure profiles of SA-Me₂ and CPH-Me₂ were characterized as a function of depth and initiating system.

Figures 6–9 report the double bond conversion as a function of depth in samples of SA-Me₂ and CPH-Me₂ polymerized with two different initiation mechanisms. The initiators included both DMPA and CQ/4EDMAB. The CQ/4EDMAB system photobleaches, which allows deeper penetration of the polymerizing light as the

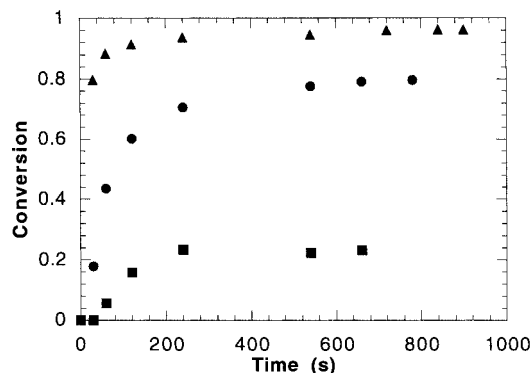


Figure 6. 3D Polymerization of SA-Me₂ with 5 mW/cm² UV light and 1.0 wt % DMPA: (▲) top; (●) 1 mm; (■) 2 mm.

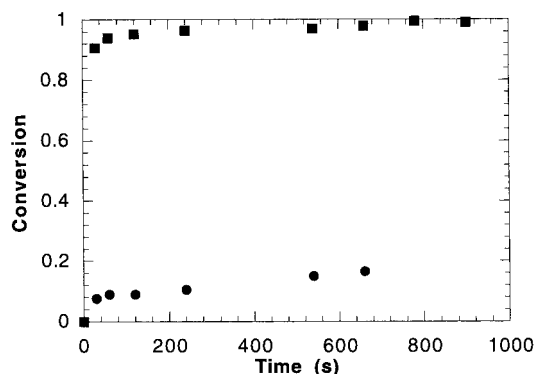


Figure 7. 3D polymerization of CPH-Me₂ using 1.0 wt % DMPA and 5 mW/cm² UV light: (■) top and (●) 1 mm.

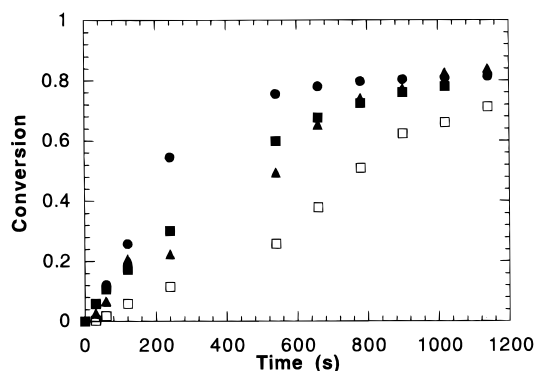


Figure 8. 3D polymerization of SA-Me₂ with 1 wt % CQ/4EDMAB at 150 mW/cm² visible light: (●) top; (■) 1 mm; (▲) 2 mm; (□) 3 mm.

absorption of the initiator decreases with exposure (i.e., the initiator bleaches).

From these figures, it is clear that both monomer systems show significant differences in the conversion profiles as a function of depth. Differences in the polymerization profile with distance from the incident light arise from many factors. For example, an initial lag period develops and becomes more pronounced at greater distances from the illuminated surface. The lag period is predominantly the result of oxygen inhibition; oxygen's affinity for free radicals combined with the lower rate of initiation allows it to compete effectively with propagation by radical quenching (precludes propagation) or peroxy radical formation (less reactive). While oxygen is present ubiquitously throughout the polymerization environment, its effects are more pronounced farther from the surface since the initiation rate is much lower.

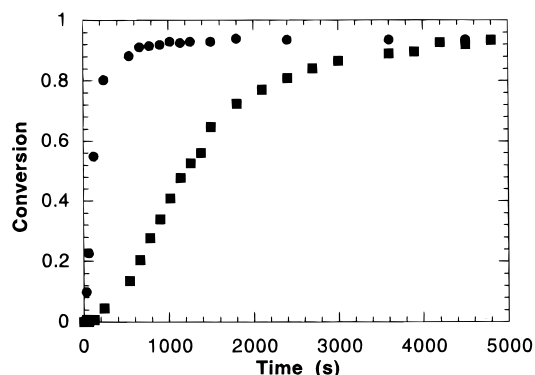


Figure 9. 3D polymerization of CPH-Me₂ using 1.0 wt % CQ/4EDMAB and 150 mW/cm² visible light: (●) top; (■) 1 mm.

In addition, Figures 6 and 7 emphasize the challenges of polymerizing thick samples with nonbleaching, UV initiators. Systems polymerized with DMPA showed significant deviation in the maximum final double bond conversion reached at the top and bottom surfaces. For example after 900 s of polymerization of SA-Me₂, double bond conversion at the top surface exceeded 96%, conversion 1 mm into the sample was only 80%, and that 2 mm into the sample dropped dramatically to 23%. The problem of light attenuation in samples is further exaggerated during the polymerization of CPH-Me₂, where the monomer has a significant absorption at 365 nm and competes with DMPA for the initiating light.

While CPH-Me₂ is not easily polymerized with low UV light intensities, its desirable degradation and mechanical properties are important for the targeted applications. To this extent, the CQ/4EDMAB system was explored to improve upon the 3D curing of these networks. In general, this initiator allowed an improved depth of cure for all of the monomers studied. Higher conversions were reached at depths of 3 mm in SA-Me₂ (surface = 82%, 3 mm = 73%) and 1 mm in CPH-Me₂ (surface = 94%, 1 mm = 93%).

For the CQ/4EDMAB initiating system, the absorbance of the initiator at 470–490 nm leads to light attenuation such that only 90% of the light is transmitted at a depth of 1 mm, 74% at 3 mm, and 61% at 5 mm. However, as the system is exposed to the initiating light, the initiator decays and photobleaches, leading to increased light penetration. For example, after 4 min of exposure to 150 mW/cm² of blue light, the ratio of transmitted to incident light increases to 0.94 at 1 mm, 0.83 at 3 mm, and 0.73 at 5 mm. After 12 min, these ratios increase to 0.98 at 1 mm, 0.93 at 3 mm, and 0.88 at 5 mm. Clearly, this feature is advantageous for the 3D curing of these systems, and further optimization and examination of the relative rate of bleaching to the consumption of the photoinitiator could enhance these conversions further.

The curing strategies discussed above represent valid approaches to photopolymerizing thick polymeric components which are required for the targeted orthopedic applications. However, some orthopedic applications may involve in vivo curing into crevices, which could pose additional challenges to achieving uniform illumination and, therein, uniform photoinitiation. To this extent, the potential of dual-initiating systems, such as combined redox initiators and photoinitiators, is attractive. Redox initiators, such as ammonium persulfate and sodium metabisulfite which are commonly used in pharmaceutical applications, would be good

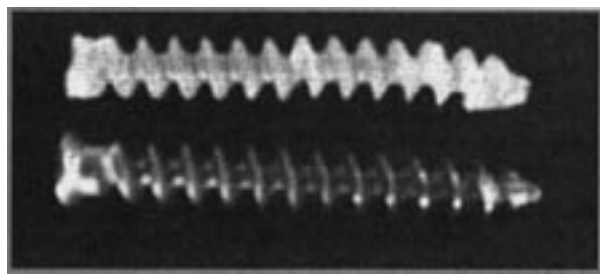


Figure 10. Prototyped polymer screw (top) photopolymerized from a mold of a metallic screw (bottom). The direction of photoinitiation was longitudinal, thus illustrating the depth of cure achieved (longest dimensions ~ 3 cm).

candidates for this type of dual-mode initiation. The dual cure-initiating mechanism offers the temporal control of the reaction afforded by the photopolymerization process along with the uniformity and completeness of cure provided by the redox polymerization. The advantages of both initiation mechanisms occurring in one system have led to advances in dentistry¹¹ and the polymerization of thick polymer composites.²⁴ Hence, by applying these techniques to our systems, we have fabricated orthopedic screw prototypes that are nearly 3 cm long (see Figure 10).

Conclusions

The polymerization behavior of two dimethacrylated anhydride monomers was investigated with varied photoinitiation schemes. In UV-initiated polymerizations, curing times were less than 2 min, and greater than 95% double bond conversion was attainable. Visible light-initiated polymerizations led to longer curing times, which were attributed mainly to the lower initiator efficiency. Many of the targeted orthopedic applications require the polymerization of complex 3D geometries, which present an additional challenge when photopolymerizing. Thus, ATR was used to study the effects of light attenuation on the depth of cure in thick samples using photobleaching and nonbleaching initiators. Using nonbleaching UV initiators, the double bond conversions at the top (illuminated) and bottom surfaces were significantly different, especially for CPH-Me₂, where the surface conversion and conversion 1 mm into the sample differed by as much as 80%. In contrast, the photobleaching capability of CQ led to increased conversion with depth in all of the systems investigated. For example, in CPH-Me₂, the surface conversion and conversion at a depth of 1 mm were nearly identical when polymerized with the photobleaching, visible light initiator. Finally, 3D prototypes of screws used in fracture fixation were fabricated using these photoinitiation schemes combined with redox initiators.

Acknowledgment. The authors would like to thank the National Science Foundation for supporting this research through a grant (BES-9741417) and to the University of Colorado Council on Research and Creative Work for a grant-in-aid.

References and Notes

- (1) Praemer, M. A.; Furner, S.; Rice, D. P. *Musculoskeletal Conditions in the United States*; AAOS: 1992.
- (2) Browner, B. D.; Jupiter, J. B.; Levine, A. M.; Trafton, P. G. *Skeletal Trauma* **1992**, 1, 42.
- (3) Bundy, K. J. In *Bone Mechanics*; Cowen, S. C., Ed.; 1989; pp 160–196.
- (4) Brighton, C. T.; Friedlaender, G.; Lane, J. M. *Bone Formation and Repair*; American Academy of Orthopedic Surgeons, Rosemont, IL, 1994.
- (5) Anseth, K. S.; Svaldi, D. C.; Laurencin, C. T.; Langer, R. In *Photopolymerization of Novel Degradable Networks for Orthopedic Applications*; Scranton, A., Bowman, C., Peiffer, R., Eds.; ACS Symposium Series 673; American Chemical Society: Washington, DC, 1997; pp 189–202.
- (6) Tortolano, F. W. *Des. News* **1996**, 70–72.
- (7) Tamada, J. A.; Langer, R. *Proc. Natl. Acad. Sci. U.S.A.* **1993**, 90, 552–556.
- (8) Kohn, D. H.; Ducheyne, P. In *Materials Science and Technology*; Cahn, R. W., Haasen, P., Kramer, E. J., Eds.; VCH: New York 1992; Vol. 14, pp 29–110. Watts, D. C. In *Materials Science and Technology*; Cahn, R. W., Haasen, P., Kramer, E. J., Eds.; VCH: New York 1992; Vol. 14, pp 209–258.
- (9) Constantz, B. *Science* **1995**, 267, 1796–1799.
- (10) Grubbs, R. H.; Coots, R. J.; Pine, S. H. US Patent 4,919,151, 1990.
- (11) Anseth, K. S.; Newman, S. M.; Bowman, C. N. *Adv. Polym. Sci.* **1995**, 122, 177–218.
- (12) Hill-West, J.; Chowdhury, S.; Sawhney, A.; Pathak, C.; Dunn, R.; Hubbell, J. *Obstet. Gynecol.* **1994**, 83, 59–64.
- (13) Steinleitner, A.; Lambert, H.; Kazensky, C.; Cantor, B. *Obstet. Gynecol.* **1991**, 77, 48–52. Steinleitner, A.; Lopez, G.; Suarez, M.; Lambert, H. *Fertil. Steril.* **1992**, 57, 305–308.
- (14) Sawhney, A. S.; Pathak, C. P.; Hubbell, J. A. *Macromolecules* **1993**, 26, 581–87.
- (15) Conix, A. *Macromol. Synth.* **1966**, 2, 95–96.
- (16) Kloosterboer, J. G. *Adv. Polym. Sci.* **1988**, 84, 1–61.
- (17) Cook, W. *Polymer* **1992**, 33, 600–609.
- (18) Anseth, K. S.; Decker, C.; Bowman, C. N. *Macromolecules* **1995**, 28, 4040–4043.
- (19) Eliades, G. C.; Voughioulakis, G. J.; Caputo, A. A. *Dent. Mater.* **1987**, 3, 19–25.
- (20) Anseth, K. S.; Kline, L. M.; Walker, T. A.; Anderson, K. J.; Bowman, C. N. *Macromolecules* **1995**, 28, 2491–2499.
- (21) Odian, G. *Principles of Polymerization*, 3rd ed.; Wiley-Interscience: New York, 1991.
- (22) Decker, C. J. *Coat. Technol.* **1987**, 59, 97–106.
- (23) Svaldi Muggli, D. C. M.S. Dissertation, Chemical Engineering Department, University of Colorado, **1997**.
- (24) Coons, L. S.; Rangarajan, B.; Godshall, D.; Scranton, A. B. In *Photopolymerizations of Vinyl Ester: Glass Fiber Composites*; Scranton, A., Bowman, C., Peiffer, R., Eds.; ACS Symposium Series 673; American Chemical Society: Washington, DC, 1997; pp 202–218.

MA980108N